Short title - **An insight into the large-scale upstream fermentation environment using scaled-down models**

Authors' names –

Corresponding Author - **Williams Olughu**, Porton Biopharma Limited, Manor Farm Road Salisbury SP4 0JG, UK, Email: williams.olughu@portonbiopharma.com, Tel: +44 (0) 1980 551545

Other Authors

Gurjot Deepika, Porton Biopharma Limited, Manor Farm Road Salisbury SP4 0JG, UK

Chris Hewitt, Aston University, Aston Triangle Birmingham B4 7ET, UK

Chris Rielly, Loughborough University, Epinal Way, Loughborough Leicestershire, LE11 3TU, UK

Key words - Scale-up, scale-down model, heterogenous cell population, large-scale inhomogeneity, high through-put fermentation, bioprocess

Nomenclature

τ_{PFR} – cell mean residence time in the plug flow reactor

τ_{STR} – cell mean residence time in the stirred tank reactor

Abbreviations

CFD - computational fluid dynamics

CT - Circulation Time

CTD - Circulation Time Distribution

DCW - dry cell weight

DO - dissolved oxygen

DOT - dissolved oxygen tension

HTP – High through-put fermentation

IPTG - Isopropyl β-D-1-thiogalactopyranoside

ldh - L-lactate dehydrogenase

mdh - malate dehydrogenase

mRNA – messenger ribonucleic acid

PFR - plug flow reactor

This article has been accepted for publication and undergone full peer review but has not been through the copyediting, typesetting, pagination and proofreading process, which may lead to differences between this version and the Version of Record. Please cite this article as doi: 10.1002/jctb.5804

ppGpp - guanosine tetraphosphate

rhGH - Human growth hormone

RTD - residence time distribution

SDR - scale-down reactors

STR - stirred tank reactor

TCA – Tricarboxylic acid

Abstract

Scaled-down models are small-scale bioreactors, used to mimic the chemical (pH, nutrient and dissolved oxygen) and physical gradients (pressure, viscosity and temperature) known to occur in the large-scale fermenter. Conventionally, before scaling up any bioprocess, small-scale bioreactors are used for strain selection, characterisation and optimisation. The typical small-scale environment is homogenous, hence all the cells held within the small-scale bioreactor can be assumed to experience the same condition at any point in time. However, for the large-scale bioreactor, this is not the case, due to its inhomogeneous environment.

Three different scaled-down models are reviewed here, and the results suggest that a bacterium responds to changes in its environment rapidly and the magnitude of response to environmental oscillations is organism-specific. The reaction and adaption of a bacterium to an inhomogeneous environment in most cases result in productivity and quality losses. This review concludes that consideration of fermentation gradients should be paramount when researchers screen for high yielding mutants in bioprocess development and doing this would help mitigate performance loss on scale-up.

1.1 Introduction

A major challenge facing bioprocess developers is the ability to accurately predict productivity, yield and quality of the large-scale fermenter from small-scale scouting studies. The level of prediction accuracy could ultimately result in the success or failure of bringing a lifesaving product to the market. Thus, the capability to simulate the large-scale fermentation environment in a small-scale bioreactor is of enormous advantage and is actively researched. This has resulted in some powerful tools, such as the development of scale-down models, which help give an insight into the complexities of the large-scale fermenter, at a reduced cost (1,2).

Typically, during the scale-up of bioprocesses certain factors such as mixing time, volumetric power input (P/V) and volumetric oxygen mass transfer coefficient ($k_L a$) to mention just a few are kept relatively constant. This is done to ensure that the final large-scale bioreactor environment is similar to that of the small-scale process development bioreactor (3). However, energy and mass transfer limitations make it impossible to maintain a constant scale-up factor as the bioreactor size increases. For example, if a 2 L STR is to be scaled-up to 20 L on the basis of $k_L a$, the energy input required for the 20 L STR to achieve similar mixing condition as the 2 L STR would be 14-fold (4,5). This cost implication makes the large-scale bioreactor design an engineering compromise, which most likely results in a suboptimal cultivation environment. Other dimensionless numbers such as Reynolds, Peclét and Froude as scale-up criteria are less popular, because of their impractical conditions and design predictions (6). Also, empirical correlations for predicting scale-up operational conditions can be useful but are limited in their applications because they are constrained to reactor geometry, impeller type, number of impellers and medium viscosity to mention but a few (6,7). These

empirical correlations typically do not consider important biological factors (i.e. metabolism, growth kinetics, transcriptional response, morphology and mutation), which if implemented could result in a universal mechanistic model accurate at predicting operating conditions on scale-up of bioprocesses (2,7,8).

The scale-up of a bioprocess usually happens towards the latter part of product development, which indicates an intention to commercialise. However, during upstream process development, small-scale bioreactors are predominantly used for characterisation. The data accumulated from these studies are then used to predict performance on scale-up. The accuracy of this prediction depends on how close the small-scale experimental environment is to that of the large-scale. In most cases these estimates fall short; hence the presumed decrease in fermentation performance (productivity, product yield and titre) on the scale-up of bioprocesses (3,9).

This problem emanates from the inherent weakness of conventional scale-up methods, which do not take into account the often inhomogeneous chemical and physical environment that cells are likely to experience in a large-scale industrial process (7,10). In contrast, process optimisation, strain screening, and predictions of productivity are often based on data collected from small-scale well-mixed fermentations, where such inhomogeneities do not exist. It is, therefore, no surprise that initial productivity based on small-scale experiments fall short when applied to larger scales. The interaction of inefficient mixing, large hydrostatic pressure changes, and low gas solubility result in a situation, where temporal and spatial gradients predominate (3). The bacterial cell's response to the presence of dissolved gas (oxygen and carbon dioxide), nutrient, metabolite and pH concentration gradients are some of the primary reasons for losses in productivity seen in the

large-scale fermentation process (11–13). Another contentious factor is shear stress damage, related to the introduction of turbines for mixing, which some researchers believe affect fermentation productivity (14). However, this study could have been misinterpreted because counter studies have shown that as long as cell sizes are smaller than the Kolmogorov microscale of turbulence, (typically for industrial microbial fermentations > 14 μm) shear damage is unlikely (15–18).

Over the years, in studying how bacterial cells respond to the large-scale fed-batch environment, some researchers have employed the use of scale-down reactors (SDR). The SDR stems from compartmentalising the large-scale fermentation environment into sections of interest (10). For example, consider the large-scale fed-batch aerobic process, with a gas sparger located at the base of the vessel and a surface feed of a highly concentrated growth medium (mainly consisting of a carbon source, such as glucose). The region around the impeller and sparger are well mixed and aerated but low in nutrients; this results in an area where the cell metabolic rate is also low. Whereas, the zone where the growth medium is fed is poorly mixed, with a limited oxygen concentration and a high carbon concentration. If there is rapid cell growth here, the formation of organic acids and stabilising proteins is increased, and the dissolved oxygen concentration is even reduced further. In processes where the medium pH is controlled, the addition of a pH controlling agent (as the cells respond to a high nutrient/low oxygen concentration) leads to a localised region of high/low pH.

Further away from these areas, towards the walls of the vessel, mixing is less efficient, creating a zone where both oxygen and carbon are limited (19). The bulk region where cells spend most of their time has an environment somewhere in between the feed addition zone and the well-mixed area of the impeller, so growth

rates adjust accordingly. Figure 1 illustrates the zones of gradients typical in a large-scale fed-batch process.

For a cell to adapt to this constantly changing environment of the large-scale fed-batch reactor (Figure 1), it typically redirects its carbon flux to maintain homoeostasis and/or switches to alternate metabolic pathways, expending resource that could have been directed towards the intended desirable product(s) (12,19).

SDRs tend to mimic the large-scale environment by segregating these zones of gradients in small-scale bioreactor(s) to study them in isolation or combination. Ultimately, the results from these exercises can then be used to predict large-scale productivity, yield and quality. The SDRs discussed and categorised here are based on the number of compartments.

1.2 One-compartment SDR

Some of the earliest works on mimicking the large-scale reactor were done in a single small-scale reactor, usually the stirred tank reactor (STR). If no thought is given to the final commercial-scale environment, it is implicitly assumed that the small-scale well-mixed reactor makes a good model. As this is not true for large-scale vessels, researchers have evaluated ways of making the one-compartment SDR a better approximation of the large-scale, e.g. by forcing time-varying operating or feed conditions in a single compartment STR (Figure 2) (20,21).

The one-compartment SDR strategy of Figure 2 was used to investigate the profile of guanosine tetraphosphate (ppGpp) as a stress response to glucose oscillations in the fed-batch fermentation of *Escherichia coli* K-12 W3110 (21). The time-varying input was glucose with an on/off period of 30 s. The results showed that glucose starvation times ≥ 30 s led to an elevated ppGpp concentration reaching 10-

fold higher than the level recorded in the control fermentation, but no dry cell weight (DCW) loss was observed (maximum DCW attained was ≈ 9.2 g/L). However, it was suggested that the effect of glucose starvation on this strain might not occur until after DCW ≥ 18 g/L (8).

The effect of glucose oscillations during a fed-batch fermentation of a recombinant strain of *E. coli* K-12 was studied using a similar one-compartment SDR strategy (the time-varying input was glucose) (22). The two feeding protocols used simulated short-term glucose starvation by equally turning off/on the glucose pump intermittently at periods of 30 s (fast cycle) and 2 min (slow cycle). The product stability, productivity and the growth rate of plasmid-free cells of these simulations were then compared to a continuous glucose fed-batch control fermentation. An α – glucosidase yield decline of 80 % was recorded as the intermittent feeding period was slowed down from 30 s to 2 min in the course of the fermentation. Although both the 30 s and 2 min glucose on/off period simulations started off with the same concentration of α – glucosidase (≈ 300 mg/L) 3 h after induction, only the 2 min glucose on/off period showed a consistent product decline to approximately 80 mg/L on termination. This indicated that α – glucosidase was significantly degraded during the slow cycle feeding fermentation. The authors suggested that the increased α – glucosidase instability was due to the elevation of the alarmone ppGpp (a stress response), which may have links to known proteolytic enzymes such as C1pP. Also, a lower number of plasmid-free cells (non-productive cells) were observed in both feeding strategies compared to the control fermentation. It was suggested that this was due to the higher transient levels of ppGpp which resulted in the better adaptation of the productive cells. This study highlighted that glucose limitation in a

large-scale fed-batch process could result in increased cell viability, but may also lead to product degradation if a critical concentration of ppGpp is exceeded.

The short-term response of *Saccharomyces cerevisiae* CEN PK 113-7D to a glucose on/off cycle was studied in a chemostat (23). The experiment was based on a 20 s glucose on and 380 s glucose off block-wise strategy in an STR of 3.9 L working volume. The report indicated a 5 % decrease in DCW and a 2-fold increase in specific acetate production (which indicates an elevated stress response), compared to the control chemostat fermentation. The pentose phosphate pathway, TCA cycle and the storage carbohydrate intermediates were also different from the control, suggesting that the bacterial cells adapted to the glucose feed gradient by modifying their metabolic pathway.

Thus, fluctuations in substrate concentration during fed-batch fermentation may result in changes in metabolic profile, improved cell viability, reduced product quality and DCW losses.

A *S. cerevisiae* NCYC 1018 strain response to dissolved oxygen (DO) gradient was compared by using three different air supply strategies – continuous, fixed periodic and the Monte Carlo cycles (24). It was argued that the Monte Carlo based cycle better represents the large-scale STR Circulation Time Distribution (CTD) compared to the fixed periodic oscillations. For the Monte Carlo simulation, the Circulation Time (CT) distribution curve was divided into 25 elements of equal probability, with each element representing a CT between 8 s and 44 s. This range of CT was chosen because it was deemed to be similar to that of a 100 m^3 STR. The total cycle time was selected at random from these 25 CTs, while the air was turned on for 5 s during each cycle. The results showed that the continuous air supply fermentation achieved the highest DCW (14.8 g/L on average), while the Monte

Carlo cycle saw a 16 % decrease in DCW and a slightly higher ethanol formation compared to the fixed periodic cycle. The increase in higher ethanol formation was attributed to DO limitation and fluctuation. They also highlighted that the difference seen between the Monte Carlo and fixed periodic cycle even with the same average CT indicated that the fermenting cells were also affected by the CTD.

The response to oxygen fluctuations during the batch cultivations of a modified *E. coli* DH5α strain was investigated using the Monte Carlo method described above (25). This strategy showed a 50 % decrease in plasmid copy number compared to the control batch fermentation (indicating an increased stress response), but no loss in either DCW or yield of β-galactosidase was observed.

The effect of DO oscillations of fixed on/off periods of 300 s, 600 s and 1200 s cycles were compared in the batch fermentation of *Kluyveromyces marxianus* NRRL-Y1109 (26). These experiments were carried out in an STR of 1 L working volume. When the 1200 s period of DO oscillations was compared to the control (no DO oscillation); no loss in DCW was recorded, but a 2.6-fold increase in ethanol and a 20 % decrease in the final β-galactosidase specific activity was seen. This difference, the authors suggested was due to DO limitation which encouraged the cells to use the fermentative pathway. The report also showed that for the 300 s DO oscillating cycle the β-galactosidase specific activity increased by 12 % when compared to the control. The authors subsequently claimed that if the magnitude of DO fluctuation was low (< 300 s), it promoted better cell adaptation, which resulted in increased β-galactosidase productivity.

The one-compartment model is easy, quick and economical to set up. However, critics highlight that in these experiments all the cells within the SDR are exposed to the same fluctuating conditions (DO or substrate fluctuations), whereas in the large-

scale fermenter different zones and CTD within the bulk flow are known to exist (27). Another limitation of this model is the difficulty of simulating real oscillations at shorter periods. A 20 s cycle DO oscillation strategy resulted in no DO fluctuation when a one-compartment SDR was used (25). Further, where nutrients were periodically dosed, no oscillatory trend was observed as illustrated in Figure 2, but rather a linear profile was seen (21–23).

1.3 Two-compartment SDR

This is currently the most widely-used model for studying the inhomogeneous conditions of the large-scale fermenter. The two forms of this model are discussed below.

1.3.1 STR/PFR configuration

This setup consists of an STR in series with a plug flow reactor (PFR) and the growth medium circulated across both reactors; Figure 3 shows a schematic of the reactor configuration. The STR environment is usually well mixed and uniform, while the PFR is the poorly mixed section where potential chemical and physical gradients may exist.

The cultivation condition in the STR is different from that of the PFR (Figure 3). The STR working volume is usually the larger of the two reactors; it is where the cell spends the most time, hence the larger range in residence time distribution (RTD). The ability to tightly control the cell mean residence time in the PFR, the relative ease of observing a cell physiological change with respect to the distance travelled along the PFR, and its flexibility, are some of the STR/PFR advantages (8,28).

A two-compartment SDR was used to impose nutrient (molasses) oscillations during the fed-batch fermentations of *S. cerevisiae*, enabling the study of this organism's metabolic response to such induced gradients (10). An aerated STR was combined with an oxygen-enriched PFR, to remove any effect of DO limitation from the study. The concentrated feed (molasses of 29.5 % w/w) was added either to the PFR or the STR in different simulations. The PFR had a volume of 850 mL, while the STR volume was 15 L. When the feed was added to the PFR, the simulation showed a 6 % loss in the final DCW compared to the control fed-batch fermentation (STR only). However, the authors claim of a higher ethanol yield (due to a higher rate of glycolysis) during their SDR simulation is debatable, because, in both the control and simulation experiments, the final concentration of ethanol returned to zero. This reduction of ethanol at the end of the process was attributed to evaporation, which is not possible as ethanol cannot completely evaporate leaving behind an aqueous broth.

In another study, a similar SDR configuration was used to investigate the effect of molasses gradients on a Baker's yeast fermentation and compared its performance to that in a 215 m^3 bubble column reactor (29). The mean cell residence time in the PFR (τ_{PFR}) set at 60 s for this SDR was claimed to match the mean circulation time of the 215 m^3 bubble column reactor. The investigators reported a 6 to 7 % loss in DCW when the SDR and the large-scale fermentations were compared to the well-mixed bench scale cultivation. They showed that ethanol production was higher in the SDR, especially during the exponential growth phase when it was approximately 1.7 times that of the control. The study also highlighted that the gassing power (ability to rise dough) of this yeast cell improved when it was cultivated in a heterogeneous environment. This increased gassing power was

recorded in both the SDR and the large-scale bubble column fermentation but not in the homogeneous small-scale STR.

The effect of limited oxygen conditions on a *Pichia pastoris* Mut+ SMD 1168 strain in batch fermentations was investigated using an SDR with a PFR volume, 10 % of the 1 L STR compartment; the τ_{PFR} simulated ranged from 1 min to 7 min (30). In this configuration, the STR was aerated, while the air entrained in the broth before entering the PFR was eliminated. This study showed that the cell's maximum specific growth rate was much more affected in the SDR (≈ 12 % loss in DCW at τ_{PFR} of 7 min) compared to the control batch process. The authors also linked the observed increase in acetate concentration to the longer τ_{PFR} in the oxygen limited PFR.

The response of an *E. coli* W3110 strain to oscillations of glucose and DO concentrations were investigated during fed-batch fermentations in an SDR, which consisted of a 10 L STR in series with a PFR of 860 mL and a mean τ_{PFR} of 113 s (31). The results indicated that when the concentrated glucose feed was added to the oxygen-restricted PFR, a 24 % decrease in DCW and a 10-fold increase in acetate concentration were observed. This response was attributed to the localised high glucose concentration and the DO limited environment of the PFR. However, in this study the feeding rate was constant, resulting in an ever-decreasing specific growth rate as the cell mass increased. This makes it difficult to compare fermentation performance across experiments in this study, because of growth rate changes as the amount of glucose available decreases.

In a large-scale bioprocess, the expression of certain genes (so-called stress genes) was used to monitor fermentation performance; this was achieved by

comparing an SDR to a 30 m^3 industrial-scale fermenter (32). The SDR consisted of an aerated 15 L STR (τ_{STR} of ≈ 9 min) in a loop with an unaerated 0.695 L PFR (τ_{PFR} of 54 s). The SDR was used to simulate both glucose gradients and glucose/DO gradients. A key finding from this work highlighted how quickly the *E. coli* W3110 strain responded to process heterogeneity such as localised high/low glucose concentrations and concomitant DO limitation, to mention but a few. For example, they showed that these cells responded to a 7 °C increase in temperature from 35 °C to 42 °C within 13 s to 15 s. In their SDR experiments, the researchers induced the synthesis of some of these so-called stress mRNAs by circulating the broth through the PFR zone, which was high in glucose and low in oxygen. They then linked the upregulation of the stress genes *ackA* mRNA to the cell's overflow metabolism (induced by high rates glycolysis), *proU* mRNA to the osmotic condition of the medium, and *frd* mRNA to oxygen availability. Interestingly in all variations of their SDRs, the stress mRNA profiles were different to that of the large-scale 30 m^3 fermenter. Although the difference in mRNA profiles indicated that their SDR was not a complete representation of the 30 m^3 STR, their work showed that these mRNA profiles could be used to monitor and evaluate the physiological state of the bacterial cells.

An STR of start-up volume of 2.5 L (rising to 4 L on termination) connected to 0.54 L PFR was used to study an *E. coli* W3110 strain response to glucose and dissolved oxygen gradients during fed-batch fermentations (33). The different degrees of this organism's physiological response were investigated from four scenarios simulated by varying the entry points of both air and glucose. In one of these simulations, the glucose and base were introduced into the unaerated PFR with a τ_{PFR} of 50 s. The authors reported a 35 % loss in DCW yield and a 15 %

increase in viability, results which were similar to that in a 20 m^3 fermentation. Based on these results, the investigators concluded that this configuration best mimicked the large-scale. Nevertheless, this conclusion might be too hasty, as there was neither data on the profile of other metabolites or transcriptional enzymes to support such an argument, which would give better evidence on the similarity of physiological response in both systems. From the additional flow cytometry results, they were able to show the *E. coli* cell membrane integrity and potential was related to its growth phase and the cultivation environment. For example, they observed that in the 20 m^3 fermentation, the population of healthy cells continually improved till the end of the process, which was contrary to the well-mixed small-scale situation. The authors inferred that process gradients somehow lead to better adapted cells, which improved viability as seen in the large-scale. They also showed that throughout the course of fermentation, healthy, depolarised and dead cells coexisted regardless of scale. This highlighted that the prevailing idea of a homogenous cell population even in a well-mixed system is questionable.

The effect of glucose and DO gradients on protein quality was studied during the fed-batch fermentations of a modified *E. coli* W3110 in a two-compartment SDR (34). The SDR had a 7 L STR working volume, which increased to 9 L at the end of the study, connected to a PFR of 0.44 L with a constant τ_{PFR} of 24 s. Their results showed that after induction, formate rapidly accumulated in all reactors regardless of scale, but in the SDR it was twice that of either the 300 L pilot-scale reactor or the 7 L control. The DCW losses in the SDR simulations ranged from 6 % to 10 %, which were attributed to the added stress of glucose and oxygen fluctuations. Counterintuitively, the quality of the product (correct growth hormone monomer formation), was highest in the SDRs, increasing on average by 10 % compared to

the well-mixed control fermentation; this abnormality was not properly addressed by the authors. However, they indicated that oxygen limitation triggered by glucose overflow was a critical parameter to the recombinant human growth hormone (*rhGH)* productivity and quality.

The effect of glucose and oxygen oscillations on a non-sporulating *Bacillus subtilis* AS3 strain was studied in an SDR, which consisted of a 10 L STR connected to an unaerated 1.2 L PFR with a constant τ_{PFR} of 60 s (35). The authors reported a 6-fold and a 2-fold increase in ethanol and arginine concentration respectively during the SDR fermentations compared to the control (STR only). This effect was attributed to an unknown re-assimilation mechanism. In all experiments, the final DCWs were similar (≈14 g/L), and no losses were recorded.

The effect of a pH gradient was studied during the batch fermentation of a *B. subtilis* AJ1992 strain by adding the base at the 50 mL PFR section of the SDR (τ_{PFR} ranged from 30 – 240 s), while the 2 L STR had a working volume of 1 L (12). The bacterial cell response to the pH variations resulted in a 27 % loss of the final product concentration (Acetoin and 2,3 – Butanediol) and a 0.75 g/L accumulation of acetic acid from zero compared to the control (STR only). This response was attributed to the bacteria cell exposure to the PFR's limited DO and fluctuating pH environment. No loss in DCW productivity was reported, which may be because the final values attained were low ≤ 4.61 g/L and any effect too small to be observed via the drying-out method.

Three chemical gradients (pH, glucose & DO) were simulated during fed-batch fermentations using an *E. coli* W3110 strain (28). In one of the simulations, where the glucose and base were added to the unaerated PFR section of τ_{PFR} = 110

s, a 71 % loss in the final DCW was observed compared to the control (STR only), but the cell viability remained high (≥ 94 %). The substantial DCW loss was attributed to the high glucose, low DO concentrations and pH fluctuations of the PFR, which led to a predominant non-proliferating dormant cell population.

The combined effect of pH, glucose and dissolved oxygen gradients were investigated on a recombinant strain of *E. coli* BL21 producing the AP50 protein, during fed-batch cultivations (36). The result indicated that the formation of the AP50 protein exerted considerable stress on the cells, which led to a 70 % DCW loss compared to the control where this protein formation was not induced. They also showed that when the cells were induced later in the process, the growth rate was 2-fold higher (a 9 h IPTG induction was compared to a 14 h IPTG induction), which meant the effect of AP50 expression was attenuated in the 14 h induction. This attenuation was claimed to be due to a reduction of IPTG concentration per cell. However, they did not quantify the actual AP50 protein levels, so could not show if the SDR simulations had any effect on productivity.

1.3.2 STR/STR configuration

The argument for this setup suggests that since stochastic mixing predominates in the large-scale vessel, it might best be mimicked by a system which has a similar Circulation Time Distribution (CTD). Thus, proponents see the STR/STR configuration as a better choice, because in both compartments a broad range of RTD can be simulated under different uniform conditions (see Figure 4). The current influx of commercial parallel STR modules (such as the DasGip© and Ambr®) is set to make this configuration popular in the future.

The metabolic profile of a cadaverine-producing *Corynebacterium glutamicum* DM1945 strain was investigated under fluctuating conditions of oxygen and glucose gradients during fed-batch fermentations using the above SDR (37). The setup consisted of an aerated STR of working volume 0.78 L in connection to an unaerated STR of 0.2 L which had a mean τ_{STR} of 3 min. There were two slightly different conditions simulated in the smaller STR. In one scenario, the DO was actively stripped with a N_2/CO_2 mix (anaerobic condition), while in the other case (no stripping was done) the smaller STR was oxygen-limited as the DO supply was from the trapped air bubbles transported from the larger STR. They reported no loss in DCW and cadaverine productivity in all simulations investigated (for all cases, the final DCW reached was ≈ 12 g/L and, cadaverine productivity was ≈ 0.22 mmol/g/h). However, they reported a significant alteration in the expression of 38 genes and 28 protein levels during the SDR experiments. They showed that the mRNA levels of L-lactate dehydrogenase (*ldh*) and malate dehydrogenase (*mdh*) increased on average 3.5-fold and 2.8-fold respectively compared to the control (STR only). This suggests the cells were responding to the oxygen limited conditions in the smaller STR. However, this increase in *ldh* and *mdh* became significant only when the trapped O_2 in the smaller STR was actively stripped out with a N_2/CO_2 mix. There was no justification for actively stripping DO except for the need to elicit a stronger cell physiological response, but doing so change the dissolution rates of gasses in the medium, which moves the SDR further away from the large-scale environment. They also argued that lactate produced in the smaller non-aerated STR was re-assimilated in the larger aerated STR. This argument is questionable because there was no mention of the glucose consumption rate. However, if the glucose feeding profile was exponential as the authors claimed, then at no point during the process was glucose

not sufficient in the larger STR, hence negating the bacterial cells need to re-assimilate lactate.

The transcriptional and metabolic levels of a modified strain of *E. coli* W3110 response to spatial dissolved oxygen gradients was investigated using an STR-STR configuration (38). The larger STR (0.8 L, τ_{STR} = 33 s) was kept anaerobic while the smaller connecting STR (0.4 L, τ_{STR} = 17 s) was maintained at a dissolved oxygen tension (DOT) of 10 %. In their batch cultivations, they observed a 30 % decrease in the specific growth rate but, a 2.4-fold increase in specific glucose uptake, which indicates an increased cell maintenance requirement. The maximum concentration of lactate and succinate increased by 53-fold and 21-fold respectively in the SDR experiments compared to the control (STR only). The analysis of the various genes transcription profile suggested that under oscillating DOT conditions the TCA cycle splits into two biosynthetic pathways. These consisted of a reductive branch producing succinyl-CoA and an oxidative branch producing 2-ketoglutarate. This indicated that *E. coli* adapted to DOT gradients by repressing the cytochrome o oxidase gene, thereby leaving the cells to utilise the less energy efficient, but high-oxygen affinity cytochrome d oxidase for respiration.

The effect of increasing circulation time (CT) on a recombinant *E. coli* W3110 strain encoded for human proinsulin was investigated using a setup made up of two STRs, an aerobic and an anaerobic compartment of 0.35 L and 0.7 L respectively (39). The response was quantified in term of DCW, productivity and by-products. The CTs were varied from 7 – 180 s, to mimic a worsening mixing scenario. The authors noted a 30 % and 94 % decrease in specific growth rate and maximum proinsulin concentration as the CT was increased to 180 s.

Substrate gradients were simulated in the chemostat fermentation of a *Penicillium chrysogenum* strain to study the effect on metabolism and penicillin productivity (20). The two connected STRs which made up the SDR used to mimic a 53,000 L commercial STR, had equal volumes of 3 L each. The substrate was fed into the STR with the ideal cultivation condition, while the other STR was substrate-limited. They observed a 39 % decrease in penicillin productivity when a τ_{STR} = 6 min was applied compared to the reference fermentation. They also compared a one-compartment SDR to this two-compartment SDR, highlighting differences in the expression levels of glucose/hexose transporter genes and penicillin gene clusters.

The two-compartment SDR is currently the most popular setup amongst researchers for studying fermentation gradients of the large-scale. This is due to its low cost, flexibility, ease of use and simplicity, to mention a few factors. However, the long-standing argument on which variant of the two-compartment model is superior remains futile and unhelpful. Investigators should make their choice based on the large-scale environment they wish to mimic. For example, top-surface additions may be better represented in an STR/PFR setup, while for subsurface additions near the impeller, the STR/STR configuration is more appropriate.

1.4 Three-compartment SDR

Recently researchers have started using three-compartment SDR models to represent different zones within a large-scale fermenter (40,41). A variant of this setup is illustrated in Figure 5.

During batch fermentations of a wild-type *C. glutamicum* strain, the CO_2/HCO^{3-} gradients of the large-scale fermenter were simulated in an STR/STR/STR three-compartment SDR (40). The transcriptional response of these

oscillations on a *C. glutamicum* ATCC13032 strain was then studied. The reactor configuration was made up of a 25 L working volume STR and two 1 L STRs connected in series. These 1 L vessels were slightly pressurised to increase the dissolved CO_2/HCO^{3-} in the medium. This was done to mimic the increased dissolution rate of CO_2/HCO^{3-} due to the high hydrostatic pressure observed in some large-scale fermenters of high aspect ratio. No loss in the specific growth rate and DCW yield were recorded, but 29 gene transcripts were altered. The most affected were cg0992 (a putative sulfate permease), cg0993 (a putative transcriptional regulator) and cg2810 (a symporter), which had a 3.58-fold, 3.34-fold and 3.53-fold increase respectively.

The effect of DO and glucose gradients on a *C. glutamicum* DM1800 strain in a two-compartment (STR/PFR) and three-compartment SDR, were compared (41). The three-compartment SDR had an STR/PFR/PFR configuration (Figure 6). In their three-compartment reactor, glucose was added to only one of the PFR, but both PFRs were unaerated; whereas for the two-compartment reactor, the PFRs (1.2 L) was unaerated, while the glucose was added to the aerated STR (10 L) section. The feeding profile was constant at 0.0017 h^{-1}, in all simulations. The results showed no difference in both DCW and lysine productivity when both SDRs were compared. Some of the metabolites, such as fumarate, aspartate, acetate, and malate, showed no difference in concentrations. Others such as glutamine, glycine and pyruvate showed slight differences. However, the lactate and succinate concentrations were two-fold higher in the three-compartment SDR.

1.5 Conclusion

From the SDRs discussed thus far, it can be inferred that the STR/PFR model is most popular amongst researchers. This is not necessarily because it is the best overall, but it offers sampling flexibility which can be correlated to different residence times across the PFR and tighter control on the cells residence time. This allows the physiology of fermenting cells to be studied quickly. The results from the few three-compartment SDR models studies indicate only a marginal value added to the understanding of how growing cells respond to large-scale fermentation heterogeneity, other than increasing the cost of experimenting (which may explain why the three-compartment model has not gained popularity amongst researchers). This is because similar information can be easily obtained from properly designed two-compartment SDR models. However, what is important to note is that none of the SDRs highlighted here actually represent the environment at the large-scale, but at best are crude approximations. Our understanding of the large-scale STR is limited, especially in large vessels > 50 m^3, where the relationship between growing cells and their environment is probably far from what is perceived currently. The interaction of factors such as gas dissolution rates (due to large hydrostatic pressures, where the solubility of gases could change by a factor of 2), gas stripping rates, growing cell, genetic modification, metabolites production, changing viscosity (due to cell growth and product increase) are just a few issues which make the large-scale environment complicated. Also, the relationship between compartment volumes and mean residence times remains unresolved, as estimating the area of interest in relation to the bulk area is difficult to measure directly. Thus, most researchers rely on computational fluid dynamics (CFD) models or experience to infer this relationship. Even if these dead zones and gradient regions were measured

directly, the dynamic environment of the large-scale STR makes it hard to accurately monitor this relationship because it constantly changes during fermentation. Hence, simulating accurate models to mimic the hydrodynamics of the large-scale is arduous. This does not mean that the present forms of SDRs available cannot be used, but expectations should be realistic. Also, these SDRs can be used effectively to select high-performing/robust mutants, map out a process operational space, study the so-called stress genes and observe a microorganism response to some of the fermentation gradients discussed thus far.

Table 1 shows all the SDR studies reviewed here, indicating the differences in cell response when the control fermentation and SDR adopted were compared. The general trend observed from these SDRs show that fermentation performance decreases as the magnitude of fermentation gradients increase. However, the level of fermentation performance decrease is organism-specific. Thus, when selecting an industrial microorganism, consideration should be given not only to high-producing strains but also the ability to thrive in the sometimes harsh large-scale fermentation environment. This is because a bacterial cell responds to changes in its environment within seconds, and fermenters with large mixing times tend to encourage chemical/physical gradients, which most likely elicit a cell stringent response (32). Hence, a high-producing strain robust to these fermentation gradients is of more economic value.

1.6 Future outlook

To increase the accuracy of SDRs in the future, the next generation of these models would have to take into consideration the inherent stochastic environment of the large-scale. For example, in the STR/PFR configuration, all the studies discussed here had a fixed τ_{PFR} held constant throughout the period of fermentation. This strategy fails to take into account that the zones of gradients when they occur in a large-scale bioreactor are not fixed spatially or temporally. To account for this, an updated strategy may consider a Monte Carlo type function used to continually vary τ_{PFR} in the course of a simulation. Also, future scaled-down models should look to studying the effect of physical gradients (such as temperature and pressure) on fermenting cells. Since commercial bioreactors typically have aspect ratios greater than one, the pressure difference between the top and bottom of such vessels may be considerable. Thus, resulting in a varying gas dissolution rates across the large-scale bioreactor, which may lead to significant changes in a cell physiological response.

The tracking of a cell lifeline around a reactor is now possible using the cell cycle model and computational fluid dynamics. The Lagrangian trajectories of 120,000 cells of *Pseudomonas putida* KT2440 travel paths were tracked for ≈260 s in a 54,000 L STR (42). These types of studies are set to improve, as computational power increases the ability to track more cells for longer times. Thus, improving the insight on how a cell's spatial and temporal position within a large-scale bioreactor from the start of life to death affects the rise of different phenotypes (43). Also, this would improve the understanding of how a bacterium travel path relates to productivity, quality and population heterogeneity in a large-scale bioreactor (9).

The advent of high through-put fermentation (HTP) platforms and robotics may help reduce bioprocess development cost/time (44). The high degree of parallelisation of HTP platforms such as microtitre plates, microfluidics bioreactor, micro-bioreactors and mini-bioreactors have enabled researchers to run large numbers of experiments within a short time (45). Hence, commercially available HTP platforms (Ambr®, BioLector® and micro-Matrix) are fast becoming the default tool for strain selection and screening, phasing-out the traditional shake flask reactor (46,47).

The BioLector® was used to select a viable strain of *P. pastoris* optimised for producing AppA phytase, which was scalable to a 0.8 L bioreactor (48). A bespoke 8-parallel mini-bioreactor successfully screened for a high $_{L}$-lactic acid-producing *Lactobacillus paracasei* strain, results which were comparable to a 5 L bioreactor (49). These are but a few examples of the current trend in early stage bioprocess development. Researchers have also adopted microfluidic technology which allows the cultivation of cells at a single-cell level. This promises even better strain characterisation and an increased understanding of cell population dynamics during fermentation (50,51). The integration of this technology has led to novel fed-batch and chemostat processes, which can handle liquid volumes in the picolitres range (52–54).

However, these HTP technologies are faced with problems of evaporation due to the small liquid volumes, coalescing air bubbles displacing liquid medium or interfering with optical probes, considerable temperature variations due to the large surface area and the lack of flexibility in aeration strategy (54). These issues indicate that the hydrodynamics of HTP platforms are significantly different from both the traditional small-scale and large-scale fermenter. Thus, for a quality-by-design

process development approach, data realised from current HTP platforms cannot be reliably used for scaling-up (44). This makes the SDRs discussed so far relevant, as they are much closer to the large-scale environment, hence applicable to scale-up studies if the right strategy is selected.

Nomenclature

τ_{PFR} – cell mean residence time in the plug flow reactor

τ_{STR} – cell mean residence time in the stirred tank reactor

Abbreviations

CFD - computational fluid dynamics

CT - Circulation Time

CTD - Circulation Time Distribution

DCW - dry cell weight

DO - dissolved oxygen

DOT - dissolved oxygen tension

HTP - Highthrough-put fermentation

IPTG - Isopropyl β-D-1-thiogalactopyranoside

ldh - L-lactate dehydrogenase

mdh - malate dehydrogenase

mRNA – messenger ribonucleic acid

PFR - plug flow reactor

ppGpp - guanosine tetraphosphate

rhGH - Human growth hormone

RTD - residence time distribution

SDR - scale-down reactors

STR - stirred tank reactor

TCA – Tricarboxylic acid

References

1. Fernandes RL, Nierychlo M, Lundin L, Pedersen a E, Puentes Tellez PE, Dutta a, et al. Experimental methods and modeling techniques for description of cell population heterogeneity. Biotechnol Adv [Internet]. 2011 [cited 2014 Jan 31];29(6):575–99. Available from: http://www.ncbi.nlm.nih.gov/pubmed/21540103
2. Noorman H. An industrial perspective on bioreactor scale-down: what we can learn from combined large-scale bioprocess and model fluid studies. Biotechnol J [Internet]. 2011 Aug [cited 2014 Jan 25];6(8):934–43. Available from: http://www.ncbi.nlm.nih.gov/pubmed/21695785
3. Lara AR, Galindo E, Ramírez OT, Palomares LA. Living with heterogeneities in bioreactors: understanding the effects of environmental gradients on cells. Mol Biotechnol [Internet]. 2006 [cited 2014 Feb 12];34(3):355–81. Available from: http://link.springer.com/article/10.1385/MB:34:3:355
4. Oldshue JY. Fermentation mixing scale-up techniques. Biotechnol Bioeng [Internet]. 1966;8(1):3–24. Available from: http://doi.wiley.com/10.1002/bit.260080103
5. Garcia F, Gomez E. Bioreactor scale-up and oxygen transfer rate in microbial processes: An overview. Biotechnol Adv [Internet]. 2009;27(2):153–76. Available from: http://dx.doi.org/10.1016/j.biotechadv.2008.10.006
6. Marques MPC, Cabral JMS, Fernandes P. Bioprocess scale-up: Quest for the parameters to be used as criterion to move from microreactors to lab-scale. J Chem Technol Biotechnol. 2010;85(9):1184–98.
7. Takors R. Scale-up of microbial processes: impacts, tools and open questions. J Biotechnol [Internet]. 2012 Jul 31 [cited 2014 Feb 5];160(1–2):3–9. Available from: http://www.ncbi.nlm.nih.gov/pubmed/22206982
8. Hewitt CJ, Nienow AW. The scale-up of microbial batch and fed-batch fermentation processes. Adv Appl Microbiol [Internet]. 2007 Jan [cited 2014 Feb 5];62(07):105–35. Available from: http://www.ncbi.nlm.nih.gov/pubmed/17869604
9. Wang G, Tang W, Xia J, Chu J, Noorman H, van Gulik WM. Integration of microbial kinetics and fluid dynamics toward model-driven scale-up of industrial bioprocesses. Eng Life Sci. 2015;15(1):20–9.
10. George S, Larsson G, Enfors S-O. A scale-down two-compartment reactor with controlled substrate oscillations: Metabolic response of Saccharomyces cerevisiae. Bioprocess Eng [Internet]. 1993;9(6):249–57. Available from: http://link.springer.com/10.1007/BF01061530
11. Xu B, Jahic M, Blomsten G. Glucose overflow metabolism and mixed-acid fermentation in aerobic large-scale fed-batch processes with Escherichia coli. 1999;564–71.
12. Amanullah A, McFarlane CM, Emery AN, Nienow AW. Scale-down model to simulate spatial pH variations in large-scale bioreactors. Biotechnol Bioeng

[Internet]. 2001 Jun 5;73(5):390–9. Available from: http://www.ncbi.nlm.nih.gov/pubmed/11320509

13. Gray DR, Chen S, Howarth W, Inlow D, Maiorella BL. CO2 in large-scale and high-density CHO cell perfusion culture. Cytotechnology. 1996;22(1–3):65–78.

14. Toma MK, Ruklisha MP, Vanags JJ, Zeltina MO, Lelte MP, Galinine NI, et al. Inhibition of microbial growth and metabolism by excess turbulence. Biotechnol Bioeng. 1991;38(5):552–6.

15. Oh SKW, Nienow a. W, Al-Rubeai M, Emery a. N. The effects of agitation intensity with and without continuous sparging on the growth and antibody production of hybridoma cells. J Biotechnol. 1989;12(1):45–62.

16. Hewitt C, Boon L, McFarlane C, Nienow A. The Use of Flow Cytometry to Study the Impact of Fluid Mechanical Stress on Escherichia coli W3110 During Continuous Cultivation in an Agitated Bioreactor. Biotechnol Lett [Internet]. 1998;27(10):612–700. Available from: http://www.ncbi.nlm.nih.gov/pubmed/10099379

17. Boswell CD, Nienow A W, Gill NK, Kocharunchitt S, Hewitt CJ. The impact of fluid mechanical stress on Saccharomyces cerevisiae cells during continuous cultivation in an agitated, aerated bioreactor; its implication for mixing in the brewing process and aerobic fermentations. 2003;81(March).

18. Chamsartra S, Hewitt C, Nienow A. The impact of fluid mechanical stress on Corynebacterium glutamicum during continuous cultivation in an agitated bioreactor. Biotechnol Lett [Internet]. 2005 May [cited 2014 Feb 4];27(10):693–700. Available from: http://www.ncbi.nlm.nih.gov/pubmed/16049736

19. Enfors SO, Jahic M, Rozkov a, Xu B, Hecker M, Jürgen B, et al. Physiological responses to mixing in large scale bioreactors. J Biotechnol [Internet]. 2001 Feb 13;85(2):175–85. Available from: http://www.ncbi.nlm.nih.gov/pubmed/11165362

20. Wang G, Zhao J, Haringa C, Tang W, Xia J, Chu J, et al. Comparative performance of different scale-down simulators of substrate gradients in Penicillium chrysogenum cultures: the need of a biological systems response analysis. Microb Biotechnol. 2018;11(3):486–97.

21. Neubauer P, Åhman M, Törnkvist M, Larsson G, Enfors SO. Response of guanosine tetraphosphate to glucose fluctuations in fed-batch cultivations of Escherichia coli. J Biotechnol. 1995;43(3):195–204.

22. Lin HY, Neubauer P. Influence of controlled glucose oscillations on a fed-batch process of recombinant Escherichia coli. J Biotechnol [Internet]. 2000 Apr 14;79(1):27–37. Available from: http://www.ncbi.nlm.nih.gov/pubmed/10817339

23. Suarez-Mendez C, Sousa A, Heijnen J, Wahl A. Fast “Feast/Famine” Cycles for Studying Microbial Physiology Under Dynamic Conditions: A Case Study with Saccharomyces cerevisiae. Metabolites [Internet]. 2014;4(2):347–72. Available from: http://www.mdpi.com/2218-1989/4/2/347/

24. Namdev PK, P Y, Murray G, B T. Experimental simulation of large-scale

bioreactor environments using Monte Carlo method. Can J Chem Eng. 1991;69(2):513–9.

25. Namdev PK, Irwin N, Thompson BG, Gray MR. Effect of Oxygen Fluctuations on Recombinant Escherichia coli Fermentation. 1993;41:666–70.

26. Cortés G, Trujillo-Roldán M a., Ramírez OT, Galindo E. Production of β-galactosidase by Kluyveromyces marxianus under oscillating dissolved oxygen tension. Process Biochem [Internet]. 2005 Feb [cited 2014 Mar 10];40(2):773–8. Available from: http://linkinghub.elsevier.com/retrieve/pii/S0032959204000792

27. Sweere APJ, Janse L, Kossen NWF. Experimental Simulation of Oxygen Profiles and Their Influence on Baker's Yeast Production: II. Two-Fermentor System. Biotechnol Bioeng. 1988;586:579–86.

28. Onyeaka H, Nienow A, Hewitt C. Further studies related to the scale-up of high cell density Escherichia coli fed-batch fermentations: the additional effect of a changing microenvironment when using aqueous ammonia to control pH. Biotechnol Bioeng [Internet]. 2003 Nov 20 [cited 2014 Feb 5];84(4):474–84. Available from: http://www.ncbi.nlm.nih.gov/pubmed/14574706

29. George S, Larsson G, Olsson K, Enfors S-O. Comparison of the Baker's yeast process performance in laboratory and production scale. Bioprocess Eng [Internet]. 1998 Feb 19;18(2):135–42. Available from: http://link.springer.com/10.1007/PL00008979

30. Lorantfy B, Jazini M, Herwig C. Investigation of the physiological response to oxygen limited process conditions of Pichia pastoris Mut(+) strain using a two-compartment scale-down system. J Biosci Bioeng [Internet]. 2013 Sep [cited 2014 Mar 5];116(3):371–9. Available from: http://www.ncbi.nlm.nih.gov/pubmed/23648104

31. Neubauer P, Haggstrom L, Enfors S. Influence of substrate oscillations on acetate formation and growth yield in Escherichia coli glucose limited fed - batch cultivations. Biotechnol Bioeng. 1995;47(2):139–46.

32. Schweder T, Krüger E, Xu B, Jürgen B, Blomsten G, Enfors SO, et al. Monitoring of genes that respond to process-related stress in large- scale bioprocesses. Biotechnol Bioeng. 1999;65(2):151–9.

33. Hewitt C, Von Caron N, Axelsson B, McFarlane C, Nienow A. Studies related to the scale-up of high-cell-density E. coli fed-batch fermentations using multiparameter flow cytometry: effect of a changing microenvironment with respect to glucose and dissolved oxygen concentration. Biotechnol Bioeng [Internet]. 2000 Nov 20;70(4):381–90. Available from: http://www.ncbi.nlm.nih.gov/pubmed/11005920

34. Bylund F, Castan a., Mikkola R, Veide a., Larsson G. Influence of scale-up on the quality of recombinant human growth hormone. Biotechnol Bioeng. 2000;69(2):119–28.

35. Junne S, Klingner A, Kabisch J, Schweder T, Neubauer P. A two-compartment bioreactor system made of commercial parts for bioprocess scale-down studies: impact of oscillations on Bacillus subtilis fed-batch cultivations.

Biotechnol J [Internet]. 2011 Aug [cited 2014 Mar 11];6(8):1009–17. Available from: http://www.ncbi.nlm.nih.gov/pubmed/21751400

36. Hewitt C, Onyeaka H, Lewis G, Taylor I, Nienow A. A Comparison of High Cell Density Fed-Batch Fermentations Involving Both Induced and Non-Induced Recombinant Escherichia coli Under Well-Mixed Small-Scale and Simulated Poorly Mixed Large-Scale Conditions. 2007;96(3):495–505.

37. Limberg MH, Schulte J, Aryani T, Mahr R, Baumgart M, Bott M, et al. Metabolic profile of 1,5-diaminopentane producing Corynebacterium glutamicum under scale-down conditions: Blueprint for robustness to bioreactor inhomogeneities. Biotechnol Bioeng. 2016;114(3):560–75.

38. Lara AR, Leal L, Flores N, Gosset G, Bolívar F, Ramírez OT. Transcriptional and metabolic response of recombinant Escherichia coli to spatial dissolved oxygen tension gradients simulated in a scale-down system. Biotechnol Bioeng. 2006;93(2):372–85.

39. Sandoval E a, Gosset G, Bolívar F, Ramírez OT. Culture of Escherichia coli under dissolved oxygen gradients simulated in a two-compartment scale-down system: metabolic response and production of recombinant protein. Biotechnol Bioeng [Internet]. 2005 Feb 20 [cited 2014 Jan 27];89(4):453–63. Available from: http://www.ncbi.nlm.nih.gov/pubmed/15609273

40. Buchholz J, Graf M, Freund A, Busche T, Kalinowski J, Blombach B, et al. CO2/HCO3 perturbations of simulated large scale gradients in a scale-down device cause fast transcriptional responses in Corynebacterium glutamicum. Appl Microbiol Biotechnol. 2014;98(20):8563–72.

41. Lemoine A, Maya Martnez-Iturralde N, Spann R, Neubauer P, Junne S, Maya Martínez-Iturralde N, et al. Response of Corynebacterium glutamicum exposed to oscillating cultivation conditions in a two- and a novel three-compartment scale-down bioreactor. Biotechnol Bioeng. 2015;112(6):1220–31.

42. Kuschel M, Siebler F, Takors R. Lagrangian Trajectories to Predict the Formation of Population Heterogeneity in Large-Scale Bioreactors. Bioengineering [Internet]. 2017;4(2):27. Available from: http://www.mdpi.com/2306-5354/4/2/27

43. Lapin A, Mu D, Reuss M. Dynamic Behavior of Microbial Populations in Stirred Bioreactors Simulated with Euler - Lagrange Methods : Traveling along the Lifelines of Single Cells †. 2004;(43):4647–56.

44. Long Q, Liu X, Yang Y, Li L, Harvey L, McNeil B, et al. The development and application of high throughput cultivation technology in bioprocess development. J Biotechnol. 2014;192(PB):323–38.

45. Lattermann C, Büchs J. Microscale and miniscale fermentation and screening. Curr Opin Biotechnol. 2015;35:1–6.

46. Grunzel P, Pilarek M, Steinbrück D, Neubauer A, Brand E, Kumke MU, et al. Mini-scale cultivation method enables expeditious plasmid production in Escherichia coli. Biotechnol J. 2014;9(1):128–36.

47. Hemmerich J, Wiechert W, Oldiges M. Automated growth rate determination in

high-throughput microbioreactor systems. BMC Res Notes. 2017;10(1):1–7.

48. Eck A, Schmidt M, Hamer S, Ruff AJ, Förster J, Schwaneberg U, et al. Improved microscale cultivation of Pichia pastoris for clonal screening. Fungal Biol Biotechnol [Internet]. 2018;5(1):8. Available from: https://fungalbiolbiotech.biomedcentral.com/articles/10.1186/s40694-018-0053-6

49. Tian X, Zhou G, Wang W, Zhang M, Hang H, Mohsin A, et al. Application of 8 ‐ parallel micro ‐ bioreactor system with non ‐ invasive optical pH and DO biosensor in high ‐ throughput screening of l ‐ lactic acid producing strain. Bioresour Bioprocess [Internet]. 2018; Available from: https://doi.org/10.1186/s40643-018-0207-7

50. Grünberger A, Wiechert W, Kohlheyer D. Single-cell microfluidics: Opportunity for bioprocess development. Vol. 29, Current Opinion in Biotechnology. 2014. p. 15–23.

51. Martins BMC, Locke JCW. Microbial individuality: how single-cell heterogeneity enables population level strategies [Internet]. Vol. 24, Current Opinion in Microbiology. Elsevier Ltd; 2015. p. 104–12. Available from: http://dx.doi.org/10.1016/j.mib.2015.01.003

52. Wang BL, Ghaderi A, Zhou H, Agresti J, Weitz DA, Fink GR, et al. Microfluidic high-throughput culturing of single cells for selection based on extracellular metabolite production or consumption. Nat Biotechnol [Internet]. 2014;32(5):473–8. Available from: http://dx.doi.org/10.1038/nbt.2857

53. Bae S, Kim CW, Choi JS, Yang J-W, Seo TS. An integrated microfluidic device for the high-throughput screening of microalgal cell culture conditions that induce high growth rate and lipid content. Anal Bioanal Chem [Internet]. 2013;405(29):9365–74. Available from: http://link.springer.com/10.1007/s00216-013-7389-9

54. Hegab HM, ElMekawy A, Stakenborg T. Review of microfluidic microbioreactor technology for high-throughput submerged microbiological cultivation. Biomicrofluidics. 2013;7(2).

List of figures

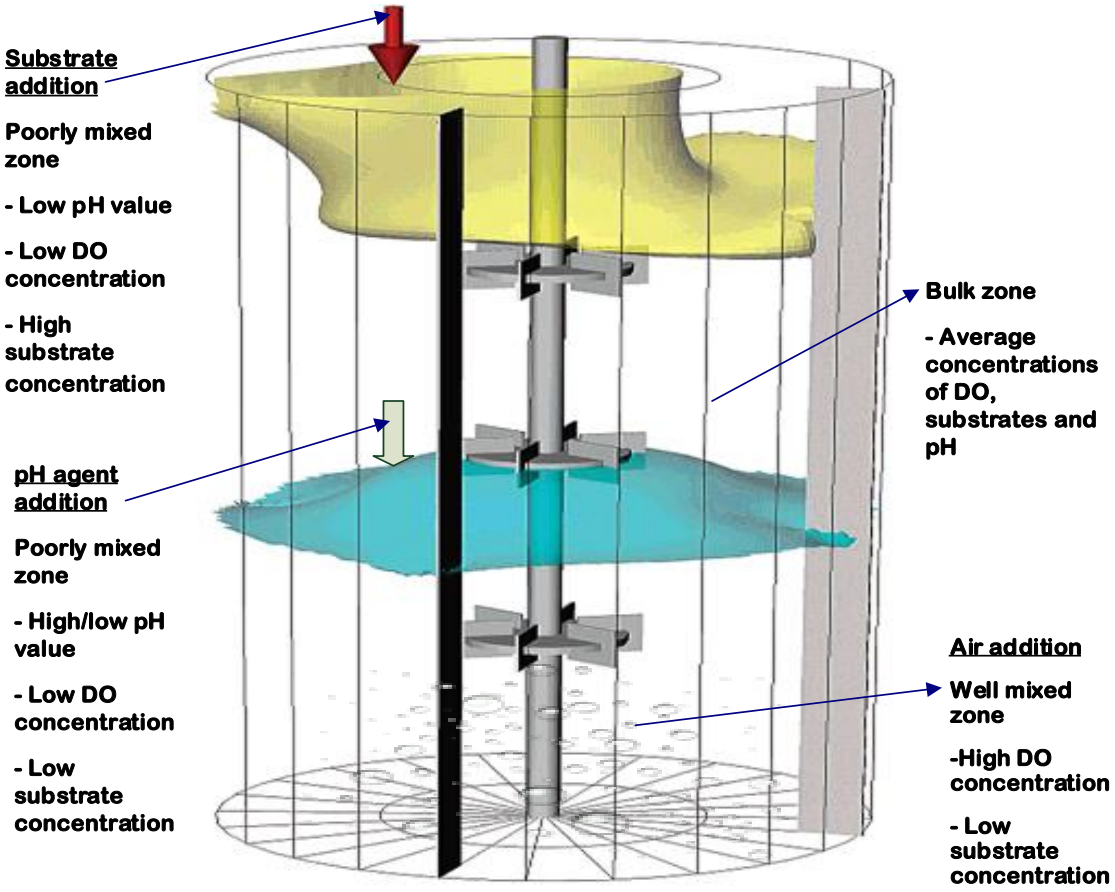

Figure 1, an overview of some zones of chemical gradients (substrate, pH and DO) that occur in the large-scale fed-batch fermentation process adapted from (43)

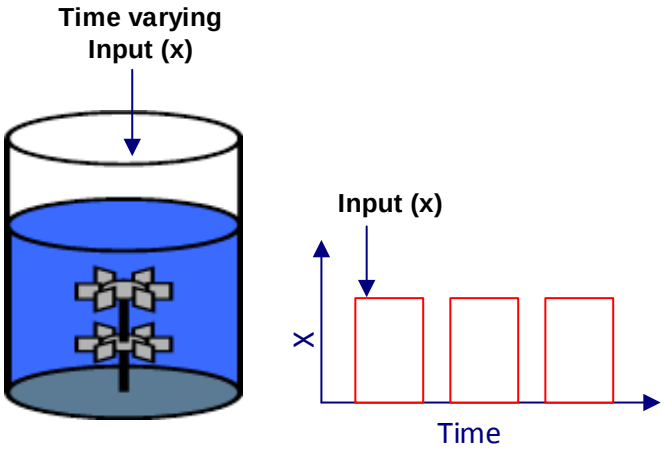

Figure 2, time-varying strategy imposed on a one-compartment reactor to mimic large-scale fermentation gradients. The input (x) may represent DO, pH or substrate addition, with the concentration profile increase and decrease corresponding to the on and off period of investigation

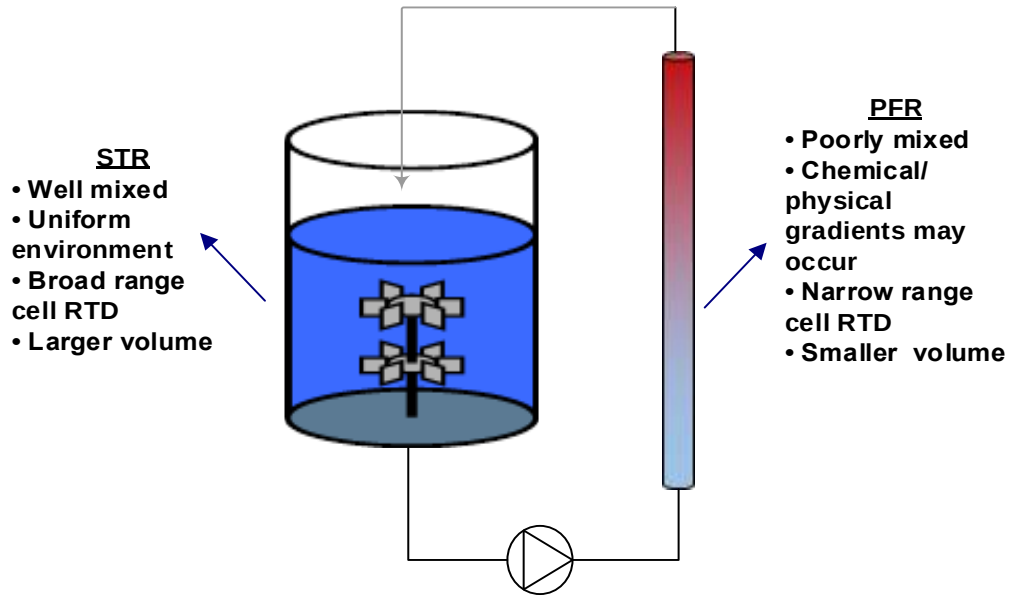

Figure 3, an STR/PFR two-compartment SDR. RTD - Residence Time Distribution. The STR represents the bulk flow region of the large-scale bioreactor, while the PFR may represent the regions of DO, substrate or pH agent addition where gradients occur

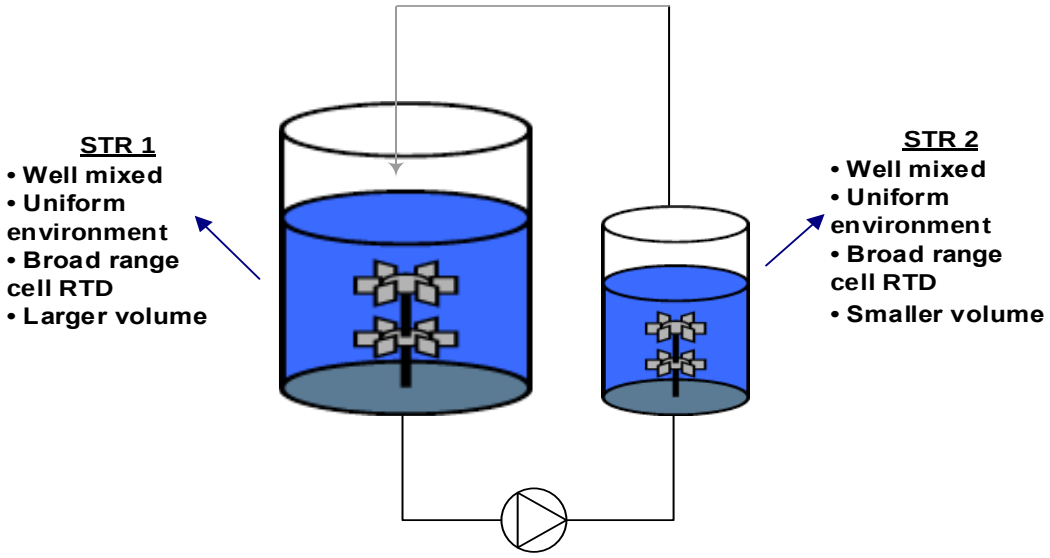

Figure 4, an STR/STR two-compartment SDR. The larger STR represents the bulk flow region of the large-scale bioreactor, while the smaller STR may represent the regions of DO, substrate or pH agent addition where gradients occur

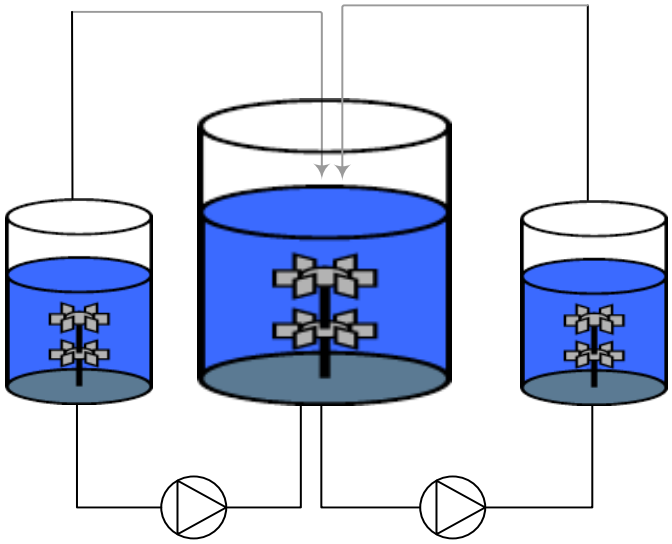

Figure 5, an STR/STR/STR three-compartment SDR. The larger STR represents the bulk flow region of the large-scale bioreactor, while the two smaller STRs may represent the regions of DO, substrate or pH agent addition where gradients occur

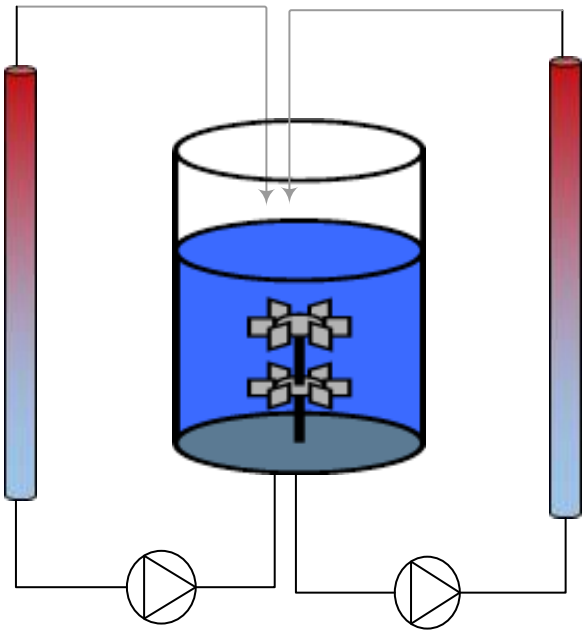

Figure 6, an STR/PFR/PFR three-compartment SDR. The STR represents the bulk flow region of the large-scale bioreactor, while the PFRs may represent the regions of DO, substrate or pH agent addition where gradients occur

List of tables

Model	Microorganism	Fermentation gradient(s) simulated	Cell response difference from control fermentation	Reference
STR	*E. coli* K-12 W3110	Glucose 30 s on-off period.	A 10-fold increase in ppGpp	(19)
STR	*E. coli* K-12	Glucose 2 min on – off period	80 % decrease in α-glucosidase	(21)
STR	*S. cerevisiae* CEN PK	Glucose 20 s on – 380 s off period	5 % decrease in DCW and a 2-fold increase in specific acetate production	(22)
STR	*S. cerevisiae* NCYC	DO Monte Carlo strategy with a CT range from 8 s to 44 s	16 % decrease in DCW and a slightly higher ethanol formation	(23)
STR	*E. coli* DH5α	DO Monte Carlo strategy with a CT range from 8 s to 44 s	50 % decrease in plasmid copy number	(24)
STR	*K. marxianus*	DO 1200 s on-off period	2.6-fold increase in ethanol formation and a 20 % decrease in β-galactosidase	(25)
STR/PFR	*S. cerevisiae*	Molasses PFR = 850 mL, STR = 15 L	6 % decrease in DCW	(7)
STR/PFR	Baker's yeast	Molasses τ_{PFR}= 60 s	6 % decrease in DCW and a 1.7-fold increase in ethanol formation	(28)
STR/PFR	*P. pastoris* Mut+	DO PFR = 100 mL, STR = 1 L, τ_{PFR} = 7 min	12 % decrease in DCW	(29)
STR/PFR	*E. coli* W3110	Glucose/DO PFR = 860 mL, STR = 10 L, τ_{PFR}= 113 s	24 % decrease in DCW and a 10-fold increase in acetate formation	(30)
STR/PFR	*E. coli* W3110	Glucose/DO PFR = 695 mL, STR = 10 L,	Upregulated *ackA*, *proU* and *frd* genes related	(31)

		τ_{PFR}= 54 s	to high glucose, osmotic condition and low DO respectively	
STR/PFR	*E. coli* W3110	Glucose/DO PFR = 540 mL, STR = 2.5 L – 4 L, τ_{PFR}= 50 s	35 % decrease in DCW and 15 % increase in viability	(32)
STR/PFR	*E. coli* W3110	Glucose/DO PFR = 440 mL, STR = 7 L – 9 L, τ_{PFR}= 24 s	10 % decrease in DCW and 10 % increase in the quality of recombinant human growth hormone	(33)
STR/PFR	*B. subtillis* AS3	Glucose/DO PFR = 1.2 L, STR = 10 L, τ_{PFR}= 60 s	6-fold and 2-fold increase in ethanol and arginine formation respectively	(34)
STR/PFR	*B. subtillis* AJ1992	pH PFR = 50 mL, STR = 1 L, τ_{PFR}= 30 s – 240 s	27 % decrease in Acetoin and 2,3 Butanediol	(10)
STR/PFR	*E. coli* W3110	Glucose/pH/DO τ_{PFR}= 110 s	71 % decrease in DCW	(27)
STR/PFR	*E. coli* BL21	Glucose/pH/DO PFR = 540 mL, STR = 2.5 L – 4 L	70 % decrease in DCW	(35)
STR/STR	*C. glutamicum* DM1945	Glucose/DO STR1 = 780 mL STR2 = 200 mL	3.5-fold and 2.8-fold increase in *ldh* and *mdh* formation	(36)
STR/STR	*E. coli* W3110	DO STR1 = 800 mL, τ_{STR1}= 33 s STR2 = 400 mL, τ_{STR2}= 17 s	30 % decrease in specific growth rate, 2.4-fold, 53-fold and 21-fold increase in specific glucose uptake, lactate and succinate formation respectively	(37)
STR/STR	*E. coli* W3110	DO STR1 = 350 mL STR2 = 700 mL CT = 180 s	30 % and 94 % decrease in specific growth rate and proinsulin titre	(38)

			respectively	
STR/STR	*P. chrysogenum*	Substrate STR1 = 3 L, STR2 = 3 L, τ_{STR}= 6 min	39 % decrease in penicillin productivity	(18)
STR/STR/STR	*C. glutamicum*	CO_2/HCO^{3-} STR1 = 25 L STR2 = 1 L STR3 = 1 L	3.6-fold, 3.3-fold and 3.5-fold increase in cg0992, cg0993 and cg2810 genes respectively	(39)
STR/PFR/PFR	*C. glutamicum* DM1800	Glucose/DO STR1 = 10 L PFR1 = 1.2 L PFR2 = 1.2 L	2-fold increase in lactate and succinate concentrations	(40)

Table 1, a summary of results from the SDRs studies reviewed